

AD-A143 466

RAMAN AND INFRARED SPECTROSCOPY OF MOLECULES ADSORBED  
ON METAL ELECTRODES(U) IBM RESEARCH LAB SAN JOSE CA  
H R PHILPOTT ET AL. JUL 84 TR-6 N00014-82-C-0583

1/1

UNCLASSIFIED

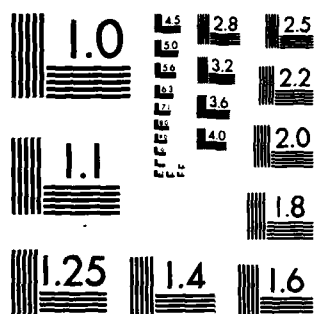
F/B 7/4

NL

END

FILMED

DTIC



MICROCOPY RESOLUTION TEST CHART  
NATIONAL BUREAU OF STANDARDS-1963-A

## REPORT DOCUMENTATION PAGE

READ INSTRUCTIONS  
BEFORE COMPLETING FORM

1. REPORT NUMBER Technical Report No. 6		2. GOVT ACCESSION NO.	3. RECIPIENT'S CATALOG NUMBER
4. TITLE (and Subtitle) Raman and Infrared Spectroscopy of Molecules Adsorbed on Metal Electrodes		5. TYPE OF REPORT & PERIOD COVERED Technical	
7. AUTHOR(s) M. R. Philpott, R. Corn, W. G. Golden, K. Kunimatsu and H. Seki		6. PERFORMING ORG. REPORT NUMBER	
9. PERFORMING ORGANIZATION NAME AND ADDRESS IBM Research Laboratory, K33/281 5600 Cottle Road San Jose, CA 95193		8. CONTRACT OR GRANT NUMBER(s) N00014-82-C0583	
11. CONTROLLING OFFICE NAME AND ADDRESS Office of Naval Research 800 North Quincy Street Arlington, VA 22217		10. PROGRAM ELEMENT, PROJECT, TASK AREA & WORK UNIT NUMBERS	
14. MONITORING AGENCY NAME & ADDRESS (if different from Controlling Office)		12. REPORT DATE July 1984	
		13. NUMBER OF PAGES 12	
		15. SECURITY CLASS. (of this report) UNCLASSIFIED	
		15a. DECLASSIFICATION/DOWNGRADING SCHEDULE	
1. DISTRIBUTION STATEMENT (of this Report) Approved for public release; distribution unlimited.			
17. DISTRIBUTION STATEMENT (of abstract entered in Block 20, if different from Report) Approved for public release; distribution unlimited.			
18. SUPPLEMENTARY NOTES Prepared for publication in Proceedings of the 17th Jerusalem Symposium in Quantum Chemistry and Biochemistry, to be published by D. Reidel Pub. Co.			
19. KEY WORDS (Continue on reverse side if necessary and identify by block number) Surface enhanced, Infrared Raman, Spectroscopy Electrode, Silver Electrolytes			
20. ABSTRACT (Continue on reverse side if necessary and identify by block number) The use of Raman and infrared spectroscopy to obtain the vibrational spectra of molecules and ions adsorbed at the metal electrode-aqueous electrolyte interface are described. To obtain Raman spectra, we use surface polaritons and roughness to enhanced spectral intensities. In the infrared, we use Fourier transform and modulated reflection-absorption techniques. Raman results for fatty acids, chloride, and thiocyanate on silver electrodes are presented, together with a combined Raman and infrared study of cyanide adsorbed on silver.			

DTIC  
ELECTE  
JUL 27 1984

B

DD FORM 1473  
1 JAN 73

SECURITY CLASSIFICATION OF THIS PAGE (When Data Entered)

84 07 25 009

AD-A143 466

FILE COPY

OFFICE OF NAVAL RESEARCH

Contract ONR-N00014-82-C-0583 NR-359-824

Raman and Infrared Spectroscopy of  
Molecules Adsorbed on Metal Electrodes

by

M. R. Philpott  
R. Corn  
W. G. Golden  
K. Kunitatsu  
H. Seki

Prepared for Publication

in

Proceedings of the 17th Jerusalem Symposium  
in Quantum Chemistry and Biochemistry

April 30 - May 3, 1984  
To be published by D. Reidel Publishing Co.

IBM Research Laboratory, K33/281

5600 Cottle Road

San Jose, California 95193

Reproduction in whole or in part is permitted for  
any purpose of the United State Government.

Approved for Public Release; Distribution Unlimited

# RAMAN AND INFRARED SPECTROSCOPY OF MOLECULES ADSORBED ON METAL ELECTRODES

M. R. Philpott, R. Corn,<sup>\*</sup> W. G. Golden,<sup>\*\*</sup> K. Kunitatsu<sup>†</sup> and H. Seki

IBM Research Laboratory, 5600 Cottle Road  
San Jose, California 95193 U.S.A.

<sup>\*</sup>Visiting scientist. Present address: Department of Chemistry, Swarthmore College, Swarthmore, Pennsylvania 19801.

<sup>\*\*</sup>IBM Instruments Inc., 40 West Brokaw Road, San Jose, California 95110.

<sup>†</sup>Visiting scientist. On leave from Research Institute of Catalysis, Hokkaido University, Sapporo, Japan.

**ABSTRACT:** The use of Raman and infrared spectroscopy to obtain the vibrational spectra of molecules and ions adsorbed at the metal electrode-aqueous electrolyte interface are described. To obtain Raman spectra, we use surface polaritons and roughness to enhanced spectral intensities. In the infrared, we use Fourier transform and modulated reflection-absorption techniques. Raman results for fatty acids, chloride, and thiocyanate on silver electrodes are presented, together with a combined Raman and infrared study of cyanide adsorbed on silver.

## I. INTRODUCTION

The vibrational spectra of molecules and ligands adsorbed at solid-liquid or solid-polymer interfaces can provide valuable information about the structure and functional properties of the interphasial region. In the last few years, techniques have been developed and phenomena discovered that make it possible to detect the IR and Raman of multilayers and even monolayers of adsorbates at these interfaces. Some examples obtained by the IBM San Jose group are described here with particular emphasis on metal electrode-aqueous electrolyte interfaces.

## II. SURFACE RAMAN SPECTROSCOPY

In vibrational Raman spectroscopy, a laser is directed at the sample and the scattered light analyzed for changes in frequency corresponding to the subtraction (Stokes scattering) or addition (anti-Stokes scattering) of a vibrational frequency. Ordinary Raman scattering is a very weak process, since

only about one photon in  $10^{10}$  is inelastically scattered. Straightforward calculations indicate that a molecular monolayer should give rise to a very small signal approximating 0.1 photons per  $\text{cm}^{-1}$  steradian watt  $\text{cm}^2$  at optical wavelengths [1]. For this reason, Raman spectroscopy was largely ignored as a tool for studying interfaces. However, in recent years, this picture has changed because of several developments. The first of these was the discovery of surface enhanced Raman scattering (SERS) from electrochemical interfaces [2-4], a variety of rough metal surfaces in vacuum and from colloidal particles [5]. The second development has been the commercial marketing of multiplex (or array) detectors which allow the recording of large spectral segments of Raman scattered light from unenhanced systems [6]. The increased theoretical understanding of electromagnetic field strengths at metal surfaces resulting from these studies has also lead to the use of surface polaritons to enhance Raman scattering processes on flat surfaces [7]. To increase the rate of Raman scattering from surface species, one can either attempt to increase the electromagnetic field amplitude or increase the cross section by tinkering with the electronic structure (e.g., create a resonance) or bonding (e.g., increase the polarizability) of the adsorbate [8].

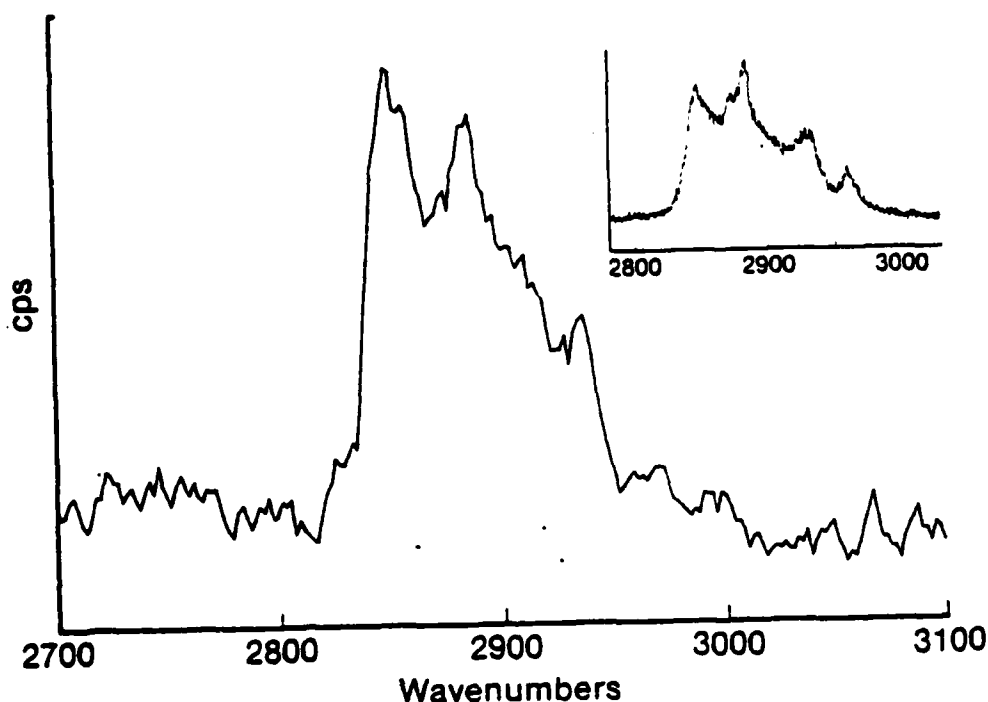


Fig. 1. PSP-enhanced spectra of the CH stretching region of 10 monolayers of cadmium arachidate at a thin silver film. Depicted in the inset for comparison is the Raman spectra from 28 monolayers deposited onto a silver grating (inset spectrum taken from Reference 11).

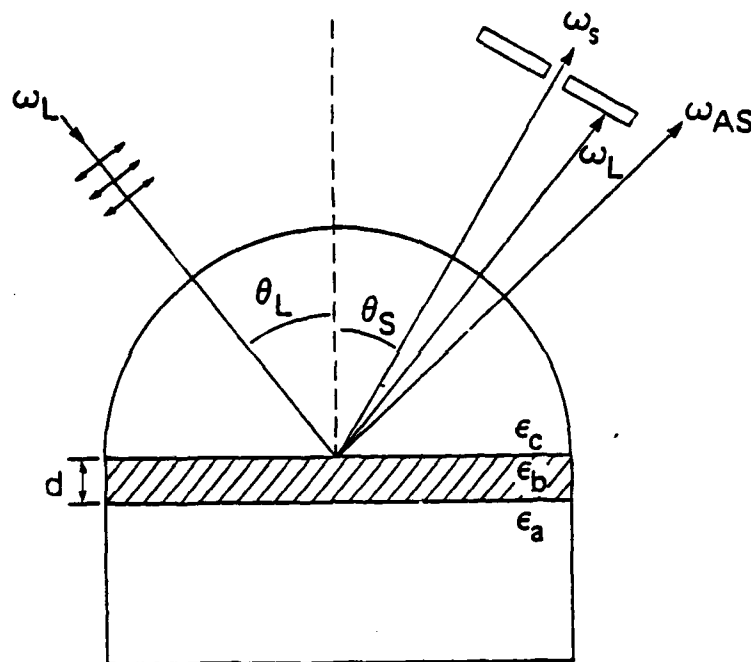


Fig. 2. Schematic diagram showing the plasmon surface polariton scattering geometry.

We describe first our method of physically enhancing the light intensity at the surface by using plasmon surface polaritons as intermediaries in the scattering process. These electromagnetic interface modes can have field amplitudes up to an order of magnitude greater than in the case of freely propagating vacuum photons. Consequently, enhancements of  $10^4$  in the cross section are possible provided surface polaritons are used as input and output channels [9-10]. This can be done by exciting surface waves on Ag, Cu or Au by grating or prism coupling [9-12]. Although grating coupling has many advantages, one drawback is the way the surfaces are made, namely, using photoresist. The resist materials is a potential source of contamination in electrochemical cells. Consequently, grating electrodes are not too convenient in electrochemical applications. On the other hand, thin films of silver on prisms can be used as working electrodes without fear of contamination since there is no photoresist layer. Figure 1 shows a Raman spectrum of ten monolayers of cadmium arachidate deposited on the flat silver film by the Langmuir-Blodgett dipping technique [9]. Figure 2 shows the experimental arrangement in a schematic fashion. In this experiment, a laser photon excites a surface polariton which undergoes Raman scattering. The scattered polaritons are then coupled out through the prism. The greater the Raman shift, the smaller is the scattering angle  $\theta_S$ . In practice,  $|\theta_L - \theta_S|$  is approximately a few degrees so that a pin hole or slit must be used to block that part of the specular beam not adsorbed by the

metal film. Rough surfaces are a serious source of scattered light at all angles too, so that the collected light must be analyzed using a conventional Raman spectrometer [9] in order to adequately reject scattered laser light.

If one tried to perform the same experiments without a grating or prism coupler, then no Raman spectrum would be detected using a conventional scanning instrument. As mentioned before, the reason for this is the absence of field enhancement due to surface plasmons. However, if one deposits on top of the Langmuir film an island film of silver, then a Raman spectrum is detectable [13,14]. The appearance of Raman scattering in this case is attributed to the presence of high electromagnetic fields around the silver particles due to localized plasma modes that can be driven at optical frequencies. These islands look very rough under SEM and mimic some aspects of electrodes that exhibit SERS.

Surface enhanced Raman scattering has received a lot of attention. As an area of study, it is beginning to mature, *i.e.*, attract lifelong devotees; however, as a phenomenon, it still remains somewhat mysterious because there seem to be several parallel enhancement mechanisms that can operate to different degrees depending on the chemical and physical characteristics of the interface. These mechanisms are roughly divisible into physical (*e.g.*, EM field enhancements at asperities or cavities) and chemical ones due to bonding that strongly couples metal and molecular polarizabilities [5,8]. In addition, there are electronic resonance effects that are voltage and wavelength dependent [15].

For silver electrodes, the metal must be subjected to an oxidation reduction cycle (ORC) that roughens the surface, creating structures capable of supporting localized plasma oscillations with frequencies in the visible. The union of these frequencies spans the visible so that at all wavelengths a SERS process occurs efficiently enough from some point on the surface for signals to be readily detected.

With multiplex detectors, one can record spectra on the millisecond time scale. By way of example, we replot some of the data published in Ref. 16. Figures 3 and 4 show the time development of SERS during an ORC. The system was Ag in contact with 0.1M NaCl and 0.01M NaSCN. The spectra in the fundamental metal-ligand M-L stretch around  $250\text{ cm}^{-1}$  and the C-N stretch at  $2100\text{ cm}^{-1}$  of the  $\text{SCN}^-$  moiety are shown separately. Detailed examination of these spectra shows a number of interesting features including displacement of  $\text{Cl}^-$  by more strongly adsorbing (but present in tenfold less concentration)  $\text{SCN}^-$  and the narrowing of the active site distribution as shown by the sharpening of the C-N stretching vibration [16].

More recently, we have looked very close to the laser line. At  $\Delta\nu \sim 10\text{ cm}^{-1}$ , there is an intense band of somewhat mysterious origins. One suggestion is that it is a particulate mode, *i.e.*, a vibration due to a surface



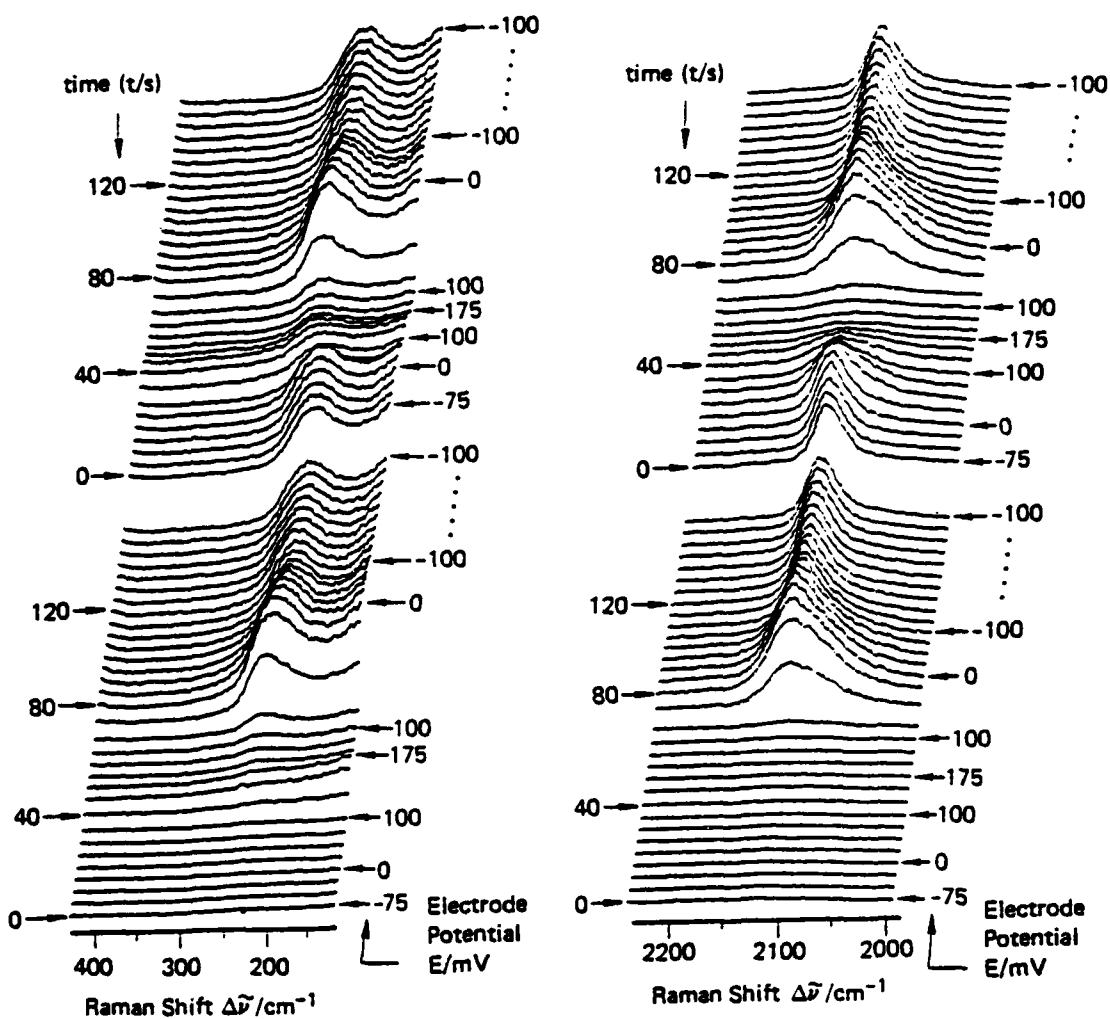


Fig. 3. (left). Time-development of SERS spectrum of a polycrystalline silver electrode in 0.1M NaCl+0.01M NaNCS during two sequential linear scan ORC from -100 mV to 175 mV and back to -100 mV at 5 mV/s. Spectra shown are for the metal-ligand bond stretching mode  $\nu_{\text{ML}}$ . Time at the beginning of each accumulation period shown on left-hand side. Electrode potential at the end of each accumulation period is shown on the right. Laser 530.9 nm, p-polarized, 200 mW. OMA accumulation period was 5 seconds for each spectrum.

Fig. 4. (right). Same electrochemical system as Figure 3. Spectra cover the range 2000 to 2200  $\text{cm}^{-1}$  which includes the C-N stretching mode  $\nu_{\text{CN}}$  of the adsorbed thiocyanate ion.

geometrical feature that contains or interacts or supports the localized plasma mode [17-18]. Experiments to understand this mode better have shown that to a first approximation at least it behaves just like the vibrational modes of

molecular adsorbates (like pyridine, for example) [19]. This implies that it is located in the vicinity of the active site itself, and is not associated solely with either a particulate or plasma mode as suggested elsewhere [17,18].

### III. SURFACE INFRARED SPECTROSCOPY

The theory on which the experimental techniques are based was developed by Greenler and others [20], who were first to note the advantage of using light near grazing incidence and the large difference in the absorption coefficient between light polarized perpendicular to the plane of reflection and that polarized parallel. Both FTIR and dispersive IR at grazing incidence were used to obtain vibrational spectra of thin films [21], Langmuir-Blodgett monolayers [14,22-25] and monolayers adsorbed on metal surfaces in ultrahigh vacuum systems [26-33]. Polarization modulation has also been explored by a number of workers as a way to improve the dynamic range of their experiment [34,35]. The spectra may be normalized to compensate for variation in intensity with wavelength if a double modulation technique is used, *i.e.*, combining polarization modulation with a second modulation scheme. By this technique, spectra of surface species may be obtained even in the presence of gas phase adsorbents. Infrared reflection absorption spectroscopy (IRRAS for short) has been demonstrated for both Fourier transform [36] and dispersion [29] spectrometers.

We have measured by Fourier transform spectroscopy the IRRAS spectrum of several systems including CO on Pt, and  $\text{CN}^-$  on Ag, Cu, Au and Pt. A thin layer electrochemical cell was used consisting of a cylindrical polycrystalline rod of metal encased in a Kel-F piston. The electrode was polished flat and moved to within a few microns of an optically flat  $\text{CaF}_2$  prism through which the IR light was directed. The cell housing was Kel-F, the reference electrode was Ag/AgCl, and the counter electrode a Pt wire. By way of example, we describe here results for  $\text{CN}^-$  adsorbed on an Ag electrode [37]. The compositions of the electrolytes used were 0.1M KCN and 0.01M KCN in 0.1M  $\text{K}_2\text{SO}_4$ .

The IRRAS spectrum includes the absorption due to the surface species and the thin layer of solution in the immediate vicinity (ca. 30 nm) of the electrode surface as described in a previous paper [38]. Consequently, there is a large background absorption due mainly to the water molecules. It is, therefore, essential to have a high signal-to-noise ratio so that this background can be subtracted out to reveal the contribution from the surface species.

The results shown in Figure 5 were obtained in the following way. First, a background spectrum was recorded for the silver electrode at -1.0V immersed in a  $\text{K}_2\text{SO}_4$  solution that did not contain any cyanide. Then cyanide was added such that a bulk concentration of 0.1N resulted. This was done with the electrode pulled back from the window. After mixing, the electrode was carefully returned to its original position. Then a series of spectra were taken with potentials between -1.4V to -0.3V and the cyanide free background

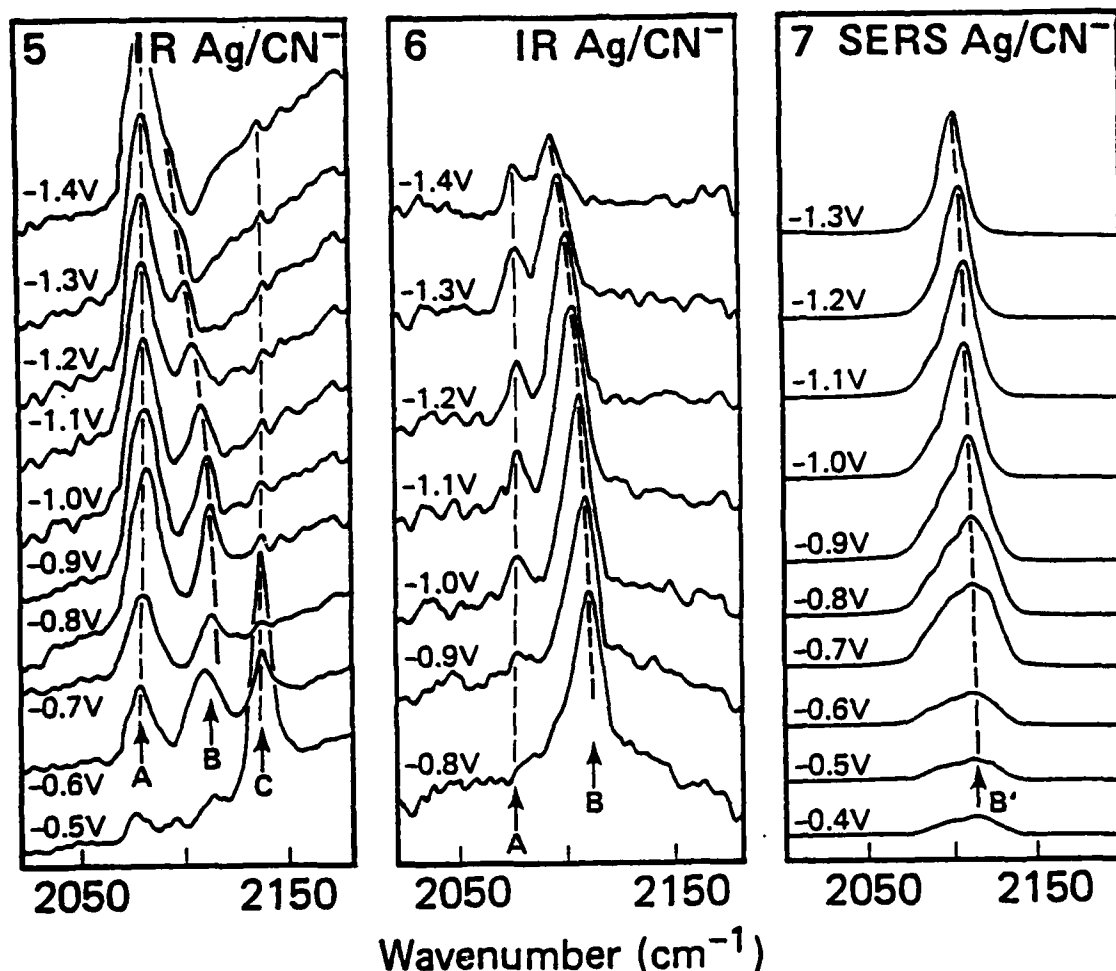


Fig. 5. (left). FT-IRRAS spectra for a solution with 0.1N  $\text{K}_2\text{SO}_4$  and 0.1N KCN. These spectra are taken starting at  $-1.4\text{V}$  (versus  $\text{Ag}/\text{AgCl}$ ). A background spectrum taken at  $-1.0\text{V}$  before adding the KCN is subtracted.

Fig. 6. (center). FT-IRRAS spectra for the same solution as for Figure 5 but using a spectrum taken at  $-1.5\text{V}$  (versus  $\text{Ag}/\text{AgCl}$ ) as the background.

Fig. 7. (right). SERS spectra taken for a solution with 0.1N  $\text{K}_2\text{SO}_4$  and 0.1N KCN after an ORC from  $-1.0$  to  $0.5\text{V}$  and back at  $50\text{ mV/sec}$ .

subtracted. Notice that at potentials more negative than  $-0.8\text{V}$ , there are two distinct bands A and B, and for potentials more positive of  $-0.7\text{V}$  there is a third band C at  $2136\text{ cm}^{-1}$ . For the lowest frequency mode A, at  $2080\text{ cm}^{-1}$  the band position and intensity remain relatively constant with potential. In contrast, the mode B continuously shifts to smaller wavenumber continuously losing its intensity with increasingly negative potential. The  $2080\text{ cm}^{-1}$  band A is assigned to the C-N stretching mode of the cyanide ions in the solution close to the electrode surface. (For a 0.1N solution, a  $1000\text{\AA}$  layer has  $6 \times 10^{14}$  solute molecules/ $\text{cm}^2$ ). The prominent band B is assigned as a surface cyanide species

since its position depends on the electrode potential and its intensity decreases as the electrode potential is made more negative. This is consistent with the surface ion desorbing as the electrode becomes negatively charged.

The surface species is desorbed at a sufficiently negative potential [39], and this suggests an alternative background subtraction method which was used to prepare the spectra shown in Figure 6. The spectra shown in Figure 6 were obtained by first taking a spectrum at  $-1.5\text{V}$  and using it as the background to subtract from the spectra taken at increasingly more positive potentials. A large part of the solution cyanide band A is eliminated by this process and the band B assigned to the surface species is more clearly revealed than in Figure 5. Notice that the bulk cyanide band is not completely subtracted. This may be due to the change in cyanide ion concentration in the diffuse layer with potential. As the potential is made more positive, the cyanide ion density increases giving more intensity and reaches a maximum between  $-1.3$  and  $-1.2\text{V}$ . Thereafter, the band intensity decreases at more positive potential due to the consumption of the cyanide ions near the electrode to produce the adsorbed surface species.

Examination of the spectra displayed in Figure 5 at potentials more positive than  $-0.6\text{V}$  shows a third band C at  $2136\text{ cm}^{-1}$  whose frequency is constant and whose intensity increases with positive potential. This band is assigned to the  $\text{Ag}(\text{CN})_2^-$  complex ion in aqueous solution. The formation of this species is accompanied by a decrease in the band B due to the surface species and a decrease in the solution cyanide peak C at  $2080\text{ cm}^{-1}$ . At increasingly positive potential, around  $-0.6\text{V}$ , the silver atoms are oxidized consuming the solution cyanide to form  $\text{Ag}(\text{CN})_2^-$  complex in the solution which is consistent with the cyclic voltammetry of this system.

The peak position of surface cyanide varies linearly with potential with a slope of about  $30\text{ cm}^{-1}/\text{volt}$  which is essentially identical to that measured for the strongest IR band of CO adsorbed on a platinum electrode [38]. The adsorption of CO on Pt has been the subject of many investigations, both in vacuum and in electrolytes. It is reasonably certain that the band at  $2080\text{ cm}^{-1}$  is due to the linearly bonded CO. Comparisons with CO on Pt electrodes raises the following questions for which we currently do not have satisfactory answers: (1) What is the nature of the bonding of  $\text{CN}^-$  to silver and how is the array of surface cyanide organized? (2) Why does the frequency shift  $30\text{ cm}^{-1}/\text{volt}$  and is the similarity with isoelectronic CO on Pt significant? (3) How does the oxidation of surface  $\text{CN}^-$  to  $\text{Ag}(\text{CN})_2^-$  take place (e.g., randomly, at defects or island edges). We expect that further work with isotopically labelled species and single crystal surfaces will answer some of these questions.

#### IV. COMPARISONS WITH SERS

We have also carried out Raman measurements in the same cell as used for the IR studies except that a fused quartz window replaced the  $\text{CaF}_2$  one [40]. The angle of incidence of the 530.8 nm Kr laser line was about  $60^\circ$  and the collection of the scattered light was normal to the laser line. There is the experimental uncertainty that it is necessary to move the electrode away from the window to carry out the ORC and returning the electrode to the exact same position is not easy. The intensity measured is slightly affected by this factor. Nevertheless, the ORC, which is required for SERS, had little effect on the IRRAS spectra.

In comparing the IRRAS results with the SERS measurements [41,42] the behavior of the C-N stretching band in the negative potential region appears to be most similar. The shift in the peak position with potential in this region has been reported to be 26 or 28  $\text{cm}^{-1}/\text{volt}$  [43,44]. In order to compare the actual band shape more closely, SERS spectra taken under conditions similar to those for the IRRAS measurements are shown in Figure 7. The OF consisted of scanning the potential to 0.5V and back to -1.0V at 50 mV/s. The SERS band is narrower at the more negative potentials and the peak position and peak shift (ca. 28  $\text{cm}^{-1}/\text{volt}$ ) is very close to those observed for the surface species with IRRAS.

Although there are similarities in the SERS and IRRAS spectra as noted above, there are also some significant differences. The intensity of the SERS band decreases more rapidly as the potential becomes more negative than -1.3V and the full width at half maximum is larger for SERS at all potentials (e.g., 20  $\text{cm}^{-1}$  versus 10  $\text{cm}^{-1}$  at -1.1V). The IR spectra return after polarizing the electrode negative whereas the SERS spectra are irreversibly lost if the potential is more negative than -1.5V. Generally, as the potential is made more positive, the SERS band shape becomes more complex and the overall bandwidth gets larger. At potentials more positive than -0.6V, the SERS band intensity decreases rapidly with increase in potential but there is no indication of bands at 2080  $\text{cm}^{-1}$  or 2136  $\text{cm}^{-1}$  due to cyanide and  $\text{Ag}(\text{CN})_2^-$  in solution as seen in the IRRAS spectra. Nor do we observe, as done by Benner *et al.* [42], the development of a very broad band peaked at 2140  $\text{cm}^{-1}$ . The conditions of their experiment were different, however, since the potential was changed rapidly, and the spectra recorded using an optical multichannel analyzer.

Briefly, our interpretation of the data presented here is as follows. The IR experiment looks at all  $\text{CN}^-$  containing surface species that can project a transition moment perpendicular to the surface. This includes a small subset of  $\text{CN}^-$  at positions where their Raman cross sections are enhanced many orders of magnitude beyond their concentration. The environment of this SERS subset is more inhomogeneous (chemically and physically) as demonstrated by the Raman linewidths and intensity dependence on potential. However, this inhomogeneity

is not so gross that the C-N stretching frequency and its dependence on electrode potential are very different. Detailed discussion of the relative merits of adatom, adcluster and cavity models for SERS *versus* simpler top site, bridged site, etc., models for IRRAS are beyond the scope of the present work.

## V. CONCLUSIONS AND OUTLOOK

There are few *in situ*, nondestructive, probes capable of providing information about the molecular structure and dynamical properties of electrochemical interfaces. The excitement following the discovery of SERS was in part connected with the expectation that it could provide a route towards formulating detailed models of the structure of the metal and accompanying Helmholtz double layer. We expect that IRRAS, to be a much more powerful tool for *in situ* probing of the electrode-electrolyte interface with the advantage that it is applicable to flat, unroughened surfaces. Supplementary techniques with some promise include second harmonic generation [45], other nonlinear spectroscopies and photoacoustic spectroscopy. Still lacking are tools that will provide accurate structural information. Even there, however, there are some expectations that surface EXAFs, surface X-ray and scanning tunneling microscopy in liquids will be available during the present decade.

## ACKNOWLEDGMENTS

We acknowledge the help and encouragement of J. G. Gordon II. This research has been supported in part by the Office of Naval Research.



Accession For	
NTIS GRA&I	<input checked="" type="checkbox"/>
DTIC TAB	<input type="checkbox"/>
Unannounced	<input type="checkbox"/>
Justification	
By	
Distribution/	
Availability Codes	
Dist	Avail and/or Special
A-1	

## REFERENCES

1. R. P. Van Duyne, in *Chemical and Biomedical Applications of Lasers*, Vol. IV, C. Bradley Moore, ed. (Academic Press, New York, 1978), Ch. 5, p. 101.
2. M. Fleischmann, P. J. Hendra and A. J. McQuillan, *Chem. Phys. Lett.* 26, 163 (1974).
3. M. G. Albrecht and J. A. Creighton, *J. Amer. Chem. Soc.* 99, 5215 (1977).
4. D. J. Jeanmaire and R. P. Van Duyne, *J. Electroanal. Chem.* 84, 1 (1977).
5. For a review, see *Surface Enhanced Raman Scattering*, R. K. Chang and T. E. Furtak, eds. (Plenum Press, New York, 1982).
6. A. Campion, J. K. Brown and V. M. Grizzle, *Surf. Sci.* 115, L153 (1982).
7. For a review of plasmon surface polaritons, see H. Raether, *Surface Plasma Oscillations and Their Applications* (Academic Press, New York-London, 1977); *Physics of Thin Films* 9, 145-261 (1976), and references therein.
8. M. R. Philpott, *J. Physique (Paris)* 44, (C10)295 (1983).
9. R. Corn and M. R. Philpott, *J. Chem. Phys.*, in press (1984).
10. S. Ushioda and Y. Sasaki, *Phys. Rev. B* 27, 1401 (1982).
11. W. Knoll, M. R. Philpott, J. D. Swalen and A. Girlando, *J. Chem. Phys.* 77, 2254-2260 (1982).
12. J. C. Tsang, J. R. Kirtley and T. N. Theis, *Solid State Commun.* 35, 667 (1980).
13. C. Y. Chen, I. Davoli, G. Ritchie and E. Burstein, *Surf. Sci.* 101, 363 (1980).
14. W. Knoll, M. R. Philpott and W. G. Golden, *J. Chem. Phys.* 77, 219 (1982).
15. A. Otto, "Surface Enhanced Raman Scattering. Classical and Chemical Origins," *Light Scattering in Solids*, Vol. IV, M. Cardona and G. Güntheradt, eds. (Springer, 1983).
16. M. R. Philpott, F. Barz, J. G. Gordon II and M. J. Weaver, *J. Electroanal. Chem.* 150, 399 (1983).
17. D. A. Weitz, J. I. Gersten and A. Z. Genack, *Phys. Rev. B* 22, 4562 (1980).
18. A. Z. Genack, D. A. Weitz and T. J. Gramila, *Surf. Sci.* 101, 381 (1980).
19. R. Corn and M. R. Philpott, *J. Chem. Phys.*, in press (1984).
20. (a) R. G. Greenler, *J. Chem. Phys.* 44, 310 (1966); (b) S. A. Francis and A. H. Ellison, *J. Opt. Soc. Amer.* 49, 131 (1959).
21. (a) P. A. Cholett, *Thin Solid Films* 52, 343 (1978); (b) R. G. Greenler, *J. Chem. Phys.* 50, 1963 (1968).
22. D. L. Allara and J. D. Swalen, *J. Phys. Chem.* 86, 2700 (1982).
23. F. A. Burns, N. E. Schlotter, J. F. Rabolt and J. D. Swalen, *IBM Instruments, Inc., Application Note No. 1* (1981).
24. T. Ohnishi, A. Ishitani, H. Ischida, N. Yamamoto and H. Tsubomura, *J. Phys. Chem.* 82, 1989 (1978).
25. W. G. Golden, C. Snyder and B. Smith, *J. Phys. Chem.* 86, 4675 (1982).
26. A. Crossley and D. A. King, *Surf. Sci.* 68, 528 (1977).
27. M. D. Baker and M. A. Chester, in *Vibrations at Surfaces*, R. Caudano et al., eds. (Plenum Press, New York, 1982).
28. H. Pfnür, D. Menzel, F. M. Hoffman, A. Ortega and A. M. Bradshaw, *Surf. Sci.* 119, 72 (1982).

29. W. G. Golden, D. S. Dunn and J. Overend, *J. Catal.* 71, 395 (1981).
30. R. Ryberg, in *Vibrations at Surfaces*, R. Caudano *et al.*, eds. (Plenum Press, New York, 1982).
31. P. Hollins and J. Pritchard, in *Vibrational Spectroscopy of Adsorbates*, R. F. Willis, ed. (Springer, New York, 1981).
32. J. C. Campuzano and R. G. Greenler, *Surf. Sci.* 83, 301 (1979).
33. M. Kawai, T. Ohnishi and K. Tamura, *Appl. Surf. Sci.* 8, 361 (1981).
34. (a) L. A. Nafie and M. Diem, *Appl. Spectrosc.* 33, 130 (1979);  
(b) L. A. Nafie, M. Diem and D. W. Vidrine, *J. Am. Chem. Soc.* 101, 496 (1979).
35. A. E. Dowry and C. Marcott, *Appl. Spectrosc.* 36, 414 (1982).
36. W. G. Golden and D. D. Saperstein, *J. Electron. Spec.* 30, 43 (1983).
37. K. Kunimatsu, H. Seki and W. G. Golden, *Chem. Phys. Lett.*, in press (1984).
38. W. G. Golden, K. Kunimatsu and H. Seki, *J. Phys. Chem.*, in press (1984).
39. N. A. Rogozhnikov and R. Yu. Bek, *Elektrokhimiya* 16, 662 (1980).
40. H. Seki, K. Kunimatsu, K. Binding, W. G. Golden, J. G. Gordon and M. R. Philpott, to be published.
41. J. Billmann, G. Kovacs and A. Otto, *Surf. Sci.* 92, 153 (1980).
42. R. E. Benner, R. Dornhaus, R. K. Chang and B. L. Laube, *Surf. Sci.* 101, 341 (1980).
43. R. Kotz and E. Yeager, *J. Electroanal. Chem.* 123, 335 (1981).
44. M. Fleischmann, I. R. Hill and M. E. Pemble, *J. Electroanal. Chem.* 136, 361 (1982).
45. R. Corn, M. Romagnoli, M. D. Levenson and M. R. Philpott, *Chem. Phys. Lett.* 106, 30 (1984).